Mixed Inter Second Order Cone Programming Taking Appropriate Approximation for the Unit Commitment in Hybrid AC-DC Grid

Zhou, Bo; Ai, Xiaomeng; Fang, Jiakun; Wen, Jingyu; Yang, Jianhua

Published in:
Journal of Engineering

DOI (link to publication from Publisher):
10.1049/joe.2017.0574

Publication date:
2017

Document Version
Accepted author manuscript, peer reviewed version

Mixed Inter Second Order Cone Programming Taking Appropriate Approximation for the Unit Commitment in Hybrid AC-DC Grid

B. Zhou[1], X.M. Ai[1], J.K. Fang[2], J.Y. Wen[1], J.H. Yang[3]

[1]State Key Laboratory of Advanced Electromagnetic Engineering and Technology (Huazhong University of Science and Technology), China, zhoubo5@hust.edu.cn, xiaomengai1986@foxmail.com, jinyu.wen@hust.edu.cn
[2]Department of Energy Technology, Aalborg University, Denmark, jiakun.fang@foxmail.com
[3]Central China Branch of State Grid Corporation of China, China

Keywords: voltage source converter, hybrid AC-DC grid; second order cone power flow constraints; unit commitment

Abstract

With the rapid development and deployment of voltage source converter (VSC) based HVDC, the traditional power system is evolving to the hybrid AC-DC grid. New optimization methods are urgently needed for these hybrid AC-DC power systems. In this paper, mixed-integer second order cone programming (MISOCP) for the hybrid AC-DC power systems is proposed. The second order cone (SOC) relaxation is adopted to transform the AC and DC power flow constraints to MISOCP. Several IEEE test systems are used to validate the proposed MISCOP formulation of the optimal power flow (OPF) and unit commitment (UC) in the hybrid AC-DC power systems.

1 Introduction

In recent years, voltage source converter based HVDC (VSC-HVDC) has drawn broad interests for its independent control of active and reactive power and improvement in commutation failure[1]. With VSC-HVDC, the multi-terminal HVDC grid (MTDC) can be formulated for its flexibility in reversing power flow[2][3]. Under this circumstances, traditional AC grid is evolving into an AC-DC hybrid grid. With HVDC links constructed, the transmission flexibility of grid get increased and some low-cost generator can replace high-cost generator to output. The power flow distribution gets optimized and the power loss and operation cost of the whole power system are decreased, which bright great economic benefits to power system[4]. Therefore, it is significant for economic operation of the power system to dispatch the hybrid AC-DC power system and make full use of the benefits brought from HVDC links. So a new optimization dispatch method for hybrid AC-DC power system are wanted.

Optimal power flow (OPF) and unit commitment (UC) are common problems for the economic operation of the power systems. But there are few studies reported on OPF or UC with VCS-HVDC. Considering the difference in component characteristics and mathematical models between VSC and current source converter (CSC), traditional OPF models of the hybrid AC-DC grid with CSC are not applicable for the hybrid AC-DC grid with VSC. And most existing studies on VSC focus on the control of VSC-based FACTS devices embedded into AC system. A few literature have studied the OPF problem of the hybrid AC-DC grid with VSC link[5]-[9]. But AC power flow constraints and detailed model of converter station are considered, and calculation methods are complicated accordingly. If the on-off states of the generators are introduced, the problem will be a mixed-inter nonconvex nonlinear programming problem. This kind of optimization problems may easily fall into the local optimum or even being intractable. So considering power flow constraints in UC with VSC-HVDC is impractical. Common UC problem considered DC power flow model in some time. However, simplification measures used in DC power flow model, especially its considering voltage at all bus as 1p.u., are not applicable for DC grid in which power transmission requires voltage difference. In [10], original nonconvex nonlinear programming problem was transformed into a second order cone programming (SOCP) problem by appropriate simplification and approximation. The SOCP problem is convex and can be solved faster by interior point method with relatively small error, and it is applicable for DC grid.

In this paper, SOC power flow constraints are introduced in UC problem and the applicability of proposed model is validated. The structure of this paper is as follow. The mathematical programming of OPF and UC is given respectively in section 2. Some case study is performed in section 3 and conclusion is given in section 4.

2 Mathematical model

2.1 Branch flow model

In [10], branch flow model has been proposed to describe the power flow of hybrid AC-DC grid. The branch flow model was transformed from traditional AC power flow model by some approximation. Compared to traditional AC power flow model, variables about line power flow were added while voltage angle variables were eliminated. Converter station model was also simplified.

2.1.1 AC line model

The equivalent model of AC lines is shown in Figure 1. j is

the index of lines. $V_{sj}e^{i\theta_{sj}}$ and $V_{rj}e^{i\theta_{rj}}$ are the voltage of sending end and receiving end, respectively. P_{sACj} and Q_{sACj} are active and reactive power flow of sending end, respectively. P_{rACj} and Q_{rACj} are active and reactive power flow of receiving end, respectively. P_{lsACj} and Q_{lsACj} are active and reactive power loss, respectively. P_{cvi} and Q_{cvi} are active and reactive power injected into AC grid from converter station, respectively. R_{lACjj}, X_{ljj} and B_{ii} are resistance, reactance, and susceptance of the line.

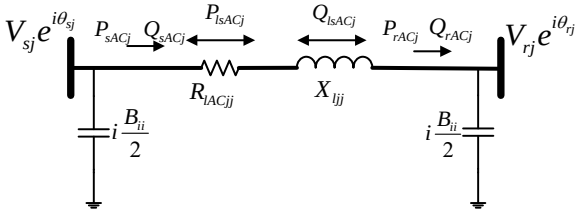

Figure 1 Equivalent model of AC lines

According to the equivalent model shown in Figure 1, the power balance equations can be obtained:

$$\begin{cases} P_{Gi} - P_{Di} + P_{cvi} = \sum_{j=1}^{n_{lAC}} M_{PQAC}(i,j) P_{rACj} + \sum_{j=1}^{n_{lAC}} M_{lAC}(i,j) P_{lsACj} \\ Q_{Gi} - Q_{Di} + Q_{cvi} = \sum_{j=1}^{n_{lAC}} M_{PQAC}(i,j) Q_{rACj} + \sum_{j=1}^{n_{lAC}} M_{lAC}(i,j) Q_{lsACj} - B_{ii} V_i^2 \end{cases} \tag{1}$$

Where M_{PQAC} and M_{lAC} are indicators for power flow directions.

$$M_{PQAC}(i,j) = \begin{cases} -1, & \text{node i is the receiving end of line j} \\ 1, & \text{node i is the sending end of line j} \\ 0, & \text{others} \end{cases} \tag{2}$$

$$M_{lAC}(i,j) = \begin{cases} 1, & \text{node i is the sending end of line j} \\ 0, & \text{others} \end{cases} \tag{3}$$

The power loss can be calculated as:

$$\frac{P_{rACj}^2 + Q_{rACj}^2}{V_{rACj}^2} R_{lACjj} = P_{lsACj} \tag{4}$$

$$\frac{P_{rACj}^2 + Q_{rACj}^2}{V_{rACj}^2} X_{ljj} = Q_{lsACj} \tag{5}$$

From (4) and (5), the relation of active and reactive power loss cab be obtained:

$$P_{lsACj} X_{ljj} = Q_{lsACj} R_{lACjj} \tag{6}$$

In addition to the power balance equations (1), the bus voltages at the sending and receiving ends can be calculated as:

$$V_{sj}e^{i\theta_{sj}} = V_{rj}e^{i\theta_{rj}} + \frac{P_{rACj} - iQ_{rACj}}{V_{rj}e^{-i\theta_{rj}}}(R_{lACjj} + iX_{ljj}) \tag{7}$$

Multiplying both sides of (7) by $V_{rj}e^{i\theta rj}$. The voltage magnitude of both sides can be calculated as:

$$\begin{aligned} V_{sj}^2 - V_{rj}^2 = {} & 2R_{lACjj}P_{rACj} + 2X_{ljj}Q_{rACj} \\ & + 2R_{lACjj}P_{lsACj} + 2X_{ljj}Q_{lsACj} \end{aligned} \tag{8}$$

Multiplying both sides of (7) by $V_{rj}e^{i\theta rj}$ and calculating its imaginary part, we can get (9) as follow:

$$V_{sj}V_{rj}\sin\theta_{srj} = X_{ljj}P_{rACj} - R_{lACjj}Q_{rACj} \tag{9}$$

Considering $sin\theta_{srj} = \theta_{srj}$ and $V_{sj}V_{rj} = 1$, (9) can be transformed into (10) as follow:

$$\theta_{srj} = X_{ljj}P_{rACj} - R_{lACjj}Q_{rACj} \tag{10}$$

Then further considering that the sum of angle difference of all lines in a loop is zero, (10) can be transformed to (11) as:

$$\sum_{k=1}^{n_C} C_{kj}X_{ljj}P_{rACj} - \sum_{k=1}^{n_C} C_{kj}R_{lACjj}Q_{rACj} = 0 \tag{11}$$

In (11), matrix C is basic loop matrix, and can be given as follow:

$$C(i,j) = \begin{cases} 1, & \text{line j is in loop i with the same direction} \\ -1, & \text{line j is in loop i with the opposite direction} \\ 0, & \text{line j is not in loop i} \end{cases} \tag{12}$$

2.1.2 DC line model

The equivalent model of DC lines is as Figure 2. The variables are similar to that of AC lines.

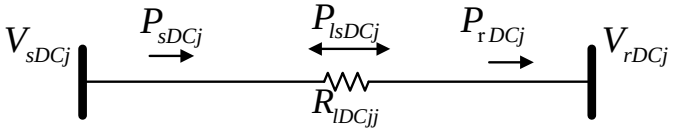

Figure 2 Equivalent model of DC lines

Power balance equation is as follow, M_{PDC} and M_{lDC} are similar to that of AC lines.

$$P_{DCi} = -\sum_{j=1}^{n_{lDC}} M_{PDC}(i,j) P_{rDCj} - \sum_{j=1}^{n_{lDC}} M_{lDC}(i,j) P_{lsDCj} \tag{13}$$

In (13), the power loss can be calculated as follow:

$$\frac{P_{rDCj}^2}{V_{rDCj}^2} R_{lDCjj} = P_{lsDCj} \tag{14}$$

In addition, the voltage equation is as:

$$V_{sDCj} = V_{rDCj} + \frac{P_{rDCj}}{V_{rDCj}} R_{lDCjj} \tag{15}$$

The square of (15) is as:

$$V_{sDCj}^2 - V_{rDCj}^2 = 2P_{rDCj}R_{DCjj} + P_{lsDCj}R_{DCjj} \tag{16}$$

2.1.3 Converter station model

In [10], the inner structure of converter station was neglected, and only power flow of both sides are considered. The equivalent model of converter station is as Figure 3. The control mode of the converter can be selected after solving OPF problem.

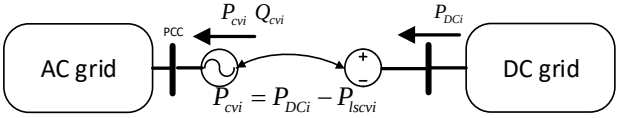

Figure 3 equivalent model of converter station

From Figure 3, power flow equation is as:

$$P_{cvi} = P_{DCi} - P_{lscvi} \tag{17}$$

In (17), power loss on converter station was considered proportional to power injected into converter station from DC grid.

$$P_{lscvi} = \beta \left| P_{cvi} \right| \tag{18}$$

2.2 SOC relaxation of the power flow constraints

From branch flow model including (1), (4), (5), (6), (8), (11), (13), (14), (16), (17) and (18), we can get power flow constraints. But there are quadratic and nonconvex constraints which will increase the calculation difficulty.

Firstly, variables representing the square of voltage are used to replace original voltage variables as follow. So (1), (8) and (16) become first-order equation.

$$W_{AC} = V_{AC}^2, \quad W_{DC} = V_{DC}^2 \tag{19}$$

Then, considering the nonconvex (4), (5) and (14), cone relaxation method is adopted and they are transformed into the convex equation as follow:

$$R_{lACjj}(P_{rACj}^2 + Q_{rACj}^2) \le P_{lsACj} W_{rACj} \tag{20}$$

$$X_{ljj}(P_{rACj}^2 + Q_{rACj}^2) \le Q_{lsACj} W_{rACj} \tag{21}$$

$$R_{lDCjj} P_{rDCj}^2 \le P_{lsDCj} W_{rDCj} \tag{22}$$

In [11], it has been revealed that such cone relaxation method is available in the radial network if angle can be recovered and line load capacity is no upper limit. In this paper, the cone relaxation method is applied in a mesh network and angle constraint is considered in (11). So angle can also be recovered. But there are upper limits in line load capacity, so we will verify the method's correctness by case study.

(18) is also a nonconvex equation. For it, square it and then relax it. The result is as:

$$\beta^2 P_{cvi}^2 \le P_{lscvi}^2 \tag{23}$$

Through above transformation, we can get the SOC power flow constraints including (1), (20), (21), (6), (8), (11), (13), (22), (16), (17), and (23).

2.3 SOCP formulation for the OPF problem in hybrid AC-DC grid

In this paper, the sum of coal cost is chosen to be the objective function, and coal cost of per generator is considered proportional to active power output. And the variables is as follow:

$$X^T = \left[P_G^T \quad Q_G^T \quad W_{AC}^T \quad P_{rAC}^T \quad Q_{rAC}^T \quad P_{lsAC}^T \quad Q_{lsAC}^T \quad P_{cv}^T \quad Q_{cv}^T \quad P_{lscv}^T \quad W_{DC}^T \quad P_{rDC}^T \quad P_{lsDC}^T \right] \tag{24}$$

The constraints of OPF is upper and lower limits of variables and SOC power flow constraints. With the SOC relaxation introduced in the previous section, the problem is an SOCP problem and can be easily solved by interior point method in commercial software such as Cplex.

2.4 MISOCP formulation for the UC problem in hybrid AC-DC grid

Common UC model usually neglects power flow constraints or considers DC power flow constraints which are not applicable for the hybrid AC-DC grid. In this paper, SOC power flow constraints are introduced to UC problem. The objective function includes coal cost, start-up and shutdown cost.

$$\text{minCost} = \sum_{t=1}^{T} \sum_{i=1}^{N_G} [b_i P_{Git} + C_{suit} + C_{sdit}] \tag{25}$$

In addition to (24), following variables are introduced.

$$\left[PU_c^T \quad PD_c^T \quad U_c^T \quad C_{su}^T \quad C_{sd}^T \right] \tag{26}$$

And the constraints combine SOC power flow constraints and other constraints proposed in paper[12]. The constraints include

1) SOC power flow constraints;
2) System spinning and operating reserve requirements;
3) Generating unit capacity;
4) Ramping up/down limits;
5) Maximum power output at up/down;
6) Minimum up/down time limits.

Therefore, the UC problem in the hybrid AC-DC grid is an MISOCP problem and can be relatively easily solved by branch and bound method and interior point method.

3 Case study on SOCP based OPF for hybrid AC-DC system

3.1 IEEE 9-BUS system

Firstly in the IEEE 9-BUS test system, we get the result of OPF considering SOC power flow constraints and compare with that using MatPower. Table 1 and Table 2 show the results.

variables	MatPower	SOC	Difference (%)
Cost ($/h)	373.83	373.85	0.0054
P_G (MW)	324.8622	324.875	0.0039
Q_G (Mvar)	46.9145	46.7228	0.41
Q_{shant} (Mvar)	158.9155	159.179	0.17
P_{loss} (MW)	9.862	9.8752	0.13
Q_{loss} (Mvar)	90.83	90.9021	0.079

Table 1 Results of different models in IEEE9 system

output	bus	MatPower	SOC	Difference (%)
Pg(MW)	1	10	10	0
	2	44.86	44.88	0.045
	3	270	270	0
Qg(Mvar)	1	26.84	28.42	5.89
	2	7.66	7.00	8.62
	3	12.41	11.30	8.94

Table 2 Output of each generator in IEEE9 system

From Table 1, the difference between the proposed SOC formulation and conventional nonlinear models in MatPower is all less than 1%. Especially, the two formulations almost obtain the same results in cost and active power output. So the

correctness of SOC power flow constraints is verified. From Table 2, the active power error of per generator is less than 0.1%, but the reactive power error of per generator is relatively larger, between 1% and 10%. The error is acceptable and according to theoretical deduction, the error may result from the approximation or the cone relaxation. Next, we verify imaginary part of the line voltage equation (7).

line	Left side	Right side	Difference (%)
1	0.0058	0.0048	16.22
2	-0.0367	-0.0316	13.89
3	-0.2224	-0.1900	14.56
4	0.1582	0.1316	16.85
5	0.1389	0.1167	15.99
6	0.0284	0.0239	15.89
7	-0.0280	-0.0233	17.07
8	0.1281	0.1101	14.05
9	-0.0363	-0.0314	13.32

Table 3 Verification for imaginary part of voltage equation

Table 3 compares the left side and the right side of equation (7) and calculates their difference. From Table 3, we can find there is a large error in imaginary part, between 10% and 20%. So we can say that the approximation of imaginary part of voltage equation is one of the error sources. Then we verify the cone relaxation through (20) and (21).

	line	Left side	Right side	Difference(%)
Active power loss (MW)	1	7.50E-06	7.50E-06	0.0203
	2	2.68E-01	2.68E-01	0.0010
	3	5.55E+00	5.55E+00	0.0010
	4	6.07E-04	6.07E-04	0.0007
	5	1.90E+00	1.90E+00	0.0010
	6	1.32E-01	1.32E-01	0.0010
	7	1.70E-06	1.70E-06	0.0006
	8	1.80E+00	1.80E+00	0.0010
	9	2.20E-01	2.20E-01	0.0010
Reactive power loss (MW)	1	4.32E-01	4.32E-01	0.0203
	2	1.45E+00	1.45E+00	0.0010
	3	2.42E+01	2.42E+01	0.0010
	4	3.56E+01	3.56E+01	0.0007
	5	1.61E+01	1.61E+01	0.0010
	6	1.12E+00	1.12E+00	0.0010
	7	1.07E+00	1.07E+00	0.0006
	8	9.08E+00	9.08E+00	0.0010
	9	1.87E+00	1.87E+00	0.0010

Table 4 Verification for relaxation of power loss equation

Table 4 compares the left side and the right side of equation (20) and (21). Table 4 show that there are same results on both sides. So cone relaxation is not the main error sources. From above analysis, the correctness of SOC power flow constraints is validated and its error mainly results from the approximation in voltage equation.

3.2 Other IEEE Test system

After verifying the correctness of SOC power flow constraints, we start to analyze its characteristic. IEEE14, IEEE30, and IEEE57 test systems are used for case study and the results are compared with DC power flow constraints and MatPower. Table 5 show the results.

From Table 5, we can find that the accuracy of SOC is much higher than that of DC in different systems and the calculation time is less than MatPower in different systems. Therefore, the SOC power flow constraints are much more accurate than DC power flow constraints and are calculated faster than MatPower.

Test system		IEEE14	IEEE30	IEEE57
Cost ($/MW)	MatPower	5371.5	5927.6	25338.1
	DC	5180	5668	25016
	SOC	5370.3	5927	25309.3
Calculation time(s)	MatPower	0.09	0.13	0.16
	DC	0.01	0.01	0.01
	SOC	0.02	0.03	0.07

Table 5 Results of different test systems

3.3 Modified IEEE 30-BUS system with DC lines

Next, the modified IEEE30 test system is used for the case study. We added five DC lines to the original IEEE30 test system, and the power system diagram is as Figure 4.

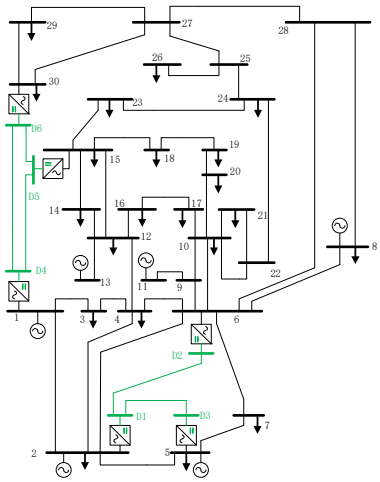

Figure 4 Modified IEEE30 system with DC links

The capacity of DC lines and converter stations is 100MW, the resistance of DC lines is 0.01p.u. , the reference voltage of DC bus is 320KV and the voltage of DC bus is between 0.94p.u. and 1.06p.u. . The results of the modified system are shown in Table 6, Table 7 and Table 8 and are compared with results of the system without DC lines.

From Table 6 and Table 7, we can find that the total cost, the output of generators and power loss of AC grid are less than that before adding DC lines. From Table 6 and Table 8, Converter stations transmit some power and power loss of DC grid exist. According to theoretical analysis, because of the economic dispatch of the power flow in the whole grid, some

system	Pure AC	Hybrid AC-DC
Cost($)	5927	5836.87
P_G(MW)	296.35	291.84
Q_G(MW)	121.41	64.04
Q_{shant}(MW)	58.948	61.04
P_{loss}(MW)	12.95	4.22
Q_{loss}(MW)	54.16	16.05
Q_{cv}(MW)	0	17.16
P_{lossDC}(MW)	0	0.4357

Table 6 Results in IEEE30 system with and without DC

Variables	AC bus	Pure AC	Hybrid AC-DC
Pg(MW)	1	156.3502	151.8436
	2	140.0000	140.0000
	5	0.0000	0.0000
	8	0.0000	0.0000
	11	0.0000	0.0000
	13	0.0000	0.0000
Qg(MW)	1	0.0000	4.8708
	2	8.2798	6.9069
	5	33.6214	6.0988
	8	39.5459	27.5902
	11	15.9650	8.0316
	13	23.9999	10.5433

Table 7 Output of each generator with and without DC

DC bus	Voltage(p.u.)	Pcv(MW)	Qcv(MW)
1	1.060	-74.0640	3.7782
2	1.058	17.2914	2.9877
3	1.055	54.2877	15.9021
4	1.060	-54.4211	-18.6728
5	1.057	37.3359	9.8445
6	1.058	15.3434	3.3247

Table 8 Detailed results of DC links

power can be transmitted through DC lines directly and so power transmitted through AC grid decreases. Considering the smaller resistance of DC lines, total power loss in the hybrid grid get decreased, so total active power output decreases and total cost decreases. On the other hand, DC lines' adding improve the flexibility of power system, so low-cost generators can replace high-cost generators to output. This can also cause the decrease of the total cost. From above analysis, the simulation results are consistent with the theoretical analysis. So we can verify the applicability of SOC power flow constraints in the hybrid AC-DC grid from the consistency between simulation results and theoretical analysis.

4 Case study on MISOCP based UC for hybrid AC-DC system

4.1 Modified IEEE 30-BUS system

In this section, we modify the IEEE30 test system in another way and use it for the case study. The modification is as follow: the maximum climbing capacity per minute of every generator is 1% of its total capacity, only generator at bus 1 is shut down at the beginning, the minimum time of start-up or shutdown is 2 hours, the maximum active power output when starting up or shutting down of generators at bus 1, 2, 5, 8, 11 and 13 is respectively 80MW, 30MW, 25MW, 25MW, 25MW and 25MW, and the start-up cost of generators at bus 1, 2, 5, 8, 11 and 13 is respectively 3000$, 3500$, 3500$, 3000$, 3000$ and 3500$. The results of MISOCP for UC problem using SOC power flow constraints in AC grid is shown in Table 9 and Figure 5 and is compared with results of MILP for UC problem using DC power flow constraints.

Model	Load (MWh)	Output (MWh)	Loss (MWh)	Coal cost ($)	Start-up cost ($)	Total cost ($)
SOC	4301	4411	110	89663	3000	92663
DC	4301	4301	0	87401	3000	90401

Table 9 Results using different UC models

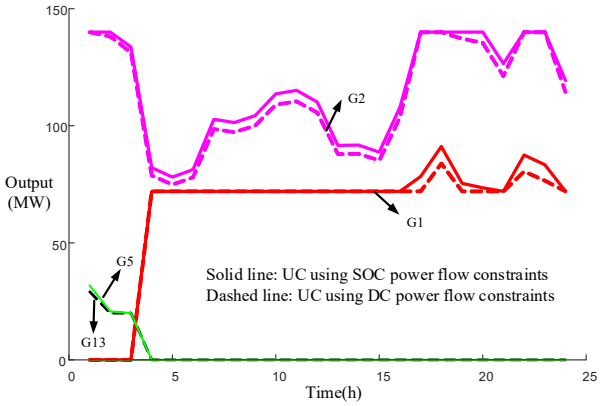

Figure 5 Output Curve of each generator using different UC models

From Table 9, the result using different power flow constraints is close and the cost using SOC constraints is a little higher than that using DC constraints. This is because power loss and reactive power are considered in SOC power flow constraints. From Figure 5, the trend of output curve is very much the same. Therefore, the proposed UC model using SOC power flow constraints is correct. Then we discuss the calculation time of the proposed UC model. The results are shown in Table 10 and are also compared with UC problem using DC constraints.

Number of time in one day		12	24	48	96
Calculation time(s)	SOC	13.88	22.67	78.33	202.98
	DC	0.022	0.14	0.359	1.349

Table 10 Calculation time using different UC models

From Table 10, with the number of time increasing, the calculation time of UC using SOC constraints is always longer than that using DC constraints. This is because SOC constraints are more complex than DC constraints.

4.2 Modified IEEE 30-BUS system with DC lines

In this section, the proposed UC model is introduced to the hybrid AC-DC grid. The IEEE30 test system is furtherly modified combining DC lines in section 3.3 and UC information in section 4.1. And a little difference from modification in section 4.1 is that generator at bus 1 is on while generator at bus 2 is off at the beginning. The result is shown in Table 11 and Figure 6 and is compared with results in pure AC grid (the load is also 4301MWh).

System	Output (MWh)	Loss (MWh)	Coal cost ($)	Start-up cost ($)	Total cost ($)
AC	4416	115	89193	3500	92693
AC-DC	4453	152	89053	0	89053

Table 11 Results using SOC constraints in pure AC grid and hybrid AC-DC grid

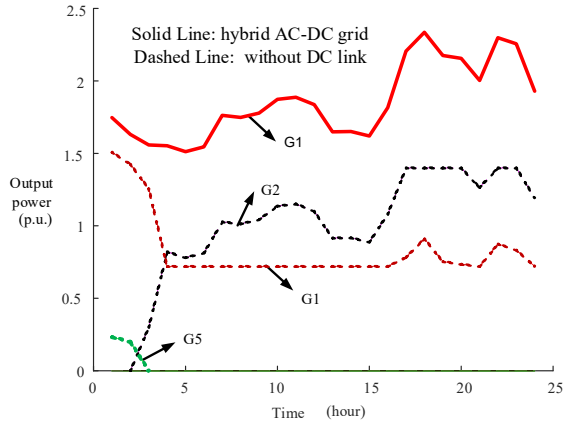

Figure 6 Output curve of each generator without and with DC links using proposed UC models

From Table 11, after DC lines added, power output and power loss increase, but coal cost, start-up cost, and total cost decrease. The reason can be gotten from Figure 6. After DC lines added, the output of G1 can satisfy all the load demand and there is no need to start up G2 and G5. Though power output and power loss are more, low-cost G1 replace high-cost G5 to output and the start-up cost of G2 is saved. So the cost gets decreased. Power from G1 can be transmitted to load bus through DC lines 4-5 and 4-6, and replace power from G2 and G5. If DC line 4-5 or 4-6 is broken, G1 cannot satisfy all the load demand and other generators must be start up. From above analysis, UC model using SOC power flow constraints is also applicable for UC problem in the hybrid AC-DC grid.

4 conclusion

In this paper, the MISOCP formulation for the OPF and UC in hybrid AC-DC power systems is proposed. The AC and DC power flow constraints are relaxed using SOC approximation. Numerical simulation validates the correctness and applicability of SOC power flow constraints in the hybrid AC-DC grid are validated in OPF model. Then its characteristic, more accurate than DC power flow constraints and faster than traditional power flow constraints, is discussed. Finally, MISOCP for UC problem considering power flow constraints in the hybrid AC-DC grid is proposed and its correctness and applicability is validated.

Acknowledgements

This work was supported in part by the China Postdoctoral Science Foundation Project (2016M590693), and in part by Central China Branch of State Grid Corporation of China.

Reference

[1] J. Yang, J. Fletcher, and J. O'Reilly, "Multi-terminal DC wind farm collection grid internal fault analysis and protection design", *IEEE Trans. Power Del.*, **vol. 25**, no. 4, pp. 2308–2318, (2010).

[2] L.X. Tang and B.-T. Ooi, "Locating and isolating DC faults in multi-terminal DC systems", *IEEE Trans. Power Del.*, **vol. 22**, no. 3, pp.1877–1884, (2007).

[3] J. Liang, T. Jing, O. Gomis-Bellmunt, J. Ekanayake, and N. Jenkins, "Operation and control of multi-terminal HVDC transmission for offshore wind farms", *IEEE Trans. Power Del.*, **vol. 26**, no. 4, pp.2596–2604, (2011).

[4] G.K. Li, Z.X. Jiang, X. Zhao, "The Characteristics and Prospect of VSC-HVDC Power Transmission", *Southern Power System Technology*, **vol. 34**, no. 9, pp.13-17, (2010).

[5] J. Yu, W. Yan, W. Li, C. Chung, and K. Wong, "An unfixed piecewise-optimal reactive power-flow model and its algorithm for AC-DC systems", *IEEE Trans. Power Syst.*, **vol. 23**, no. 1, pp. 170–176, (2008).

[6] A. Lotfjou, M. Shahidehpour, Y. Fu, "Hourly Scheduling of DC Transmission Lines in SCUC With Voltage Source Converters" , *IEEE Trans. Power Del.*, **vol. 26**, no. 2, pp. 650–660, (2011).

[7] C. Zheng, X.X. Zhou, R.M. Li. "Study on the Steady Characteristic and Algorithm of Power Flow for VSC-HVDC", *Proceedings of the CSEE*, **vol. 25**, no. 6, pp. 1-5, (2005).

[8] A. Pizano-Martinez, C.R. Fuerte-Esquivel, H. Ambriz-Perez, E. Acha. "Modelling of VSC-based HVDC systems for a Newton-Raphson OPF algorithm", *IEEE Trans. Power Del.*, **vol. 22**, no. 4, pp. 1794-1805, (2007).

[9] Z.L. Wei, C. Ji, G.Q. Song. "Interior-point Optimal Power Flow of AC-DC System with VSC-HVDC". *Proceedings of the CSEE*, **vol. 32**, no. 19, pp. 89-95, (2012).

[10] M. Baradar, M.R. Hesamzadeh, M. Ghandhari. "Second-Order Cone Programming for Optimal Power Flow in VSC-Type AC-DC Grids". *IEEE Transactions on Power Systems*, **vol. 28**, no. 4, pp. 4282-4291, (2013).

[11] M. Farivar, C. Clarke, S. Low, K. Chandy, "Inverter var control for distribution systems with renewables", *Proc. 2011 IEEE Int. Conf. Smart Grid Communications (Smart Grid Comm)*, pp. 457–462, (2011).

[12] J.H. Li, F. Lan. "The Overview on Models and Algorithms for Unit Commitment Problem", *Modern E lectric Power*, **vol. 28**, no. 6, pp. 1-10, (2011).